

Article

Extraction and Spatiotemporal Evolution Analysis of Impervious Surface and Surface Runoff in Main Urban Region of Hefei City, China

Gang Fang ^{1,2,3}, Han Li ^{1,*}, Jie Dong ¹, Hanyang Teng ¹, Renato Dan A. Pablo II ^{2,*} and Yin Zhu ¹

¹ School of Environment and Surveying Engineering, Suzhou University, Suzhou 234000, China; gangf0809@126.com (G.F.)

² Graduate School, Angeles University Foundation, Angeles 2009, Philippines

³ 3S Technology Application Research Center in Northern Anhui, Suzhou 234000, China

* Correspondence: hli020319@gmail.com (H.L.); pablo.renatodan@auf.edu.ph (R.D.A.P.II)

Abstract: The biophysical composition index (BCI)-based linear spectral mixture model (LSMM) is used in this study to extract the impervious surface (IS), vegetation, and soil coverage of the main urban region (MUR) of Hefei City over the 2001–2021 period. In addition, the Soil Conservation Service–Curve Number (SCS-CN) model is first applied to simulate the surface runoff (SR) in the MUR of Hefei City over the past 21 years, then assessed for simulation accuracy using typical waterlogging points in the study area. On this basis, the spatiotemporal evolution of IS and SR and their relationships in the MUR of Hefei City are investigated and discussed in this study. The obtained results showed that (1) the root-mean-square error (RMSE), mean absolute error (MAE), and systematic error (SE) values of the BCI index-based LSMM are smaller than those of the LSMM, demonstrating a higher extraction accuracy of urban IS extraction of the BCI index-based LSMM. (2) The IS area of the MUR of Hefei City exhibits an increasing trend from 107.555 km² in 2001 to 387.660 km² in 2021. In addition, the change rate and change intensity values indicate an increasing–decreasing–increasing trend. The highest change rate and change intensity values are 24.839 km²/year and 23.094%, respectively, and were observed in the 2001–2005 period. (3) The simulated SR (165–195 mm) in the MUR of Hefei City demonstrates an increasing trend in the 2001–2021 period at a rainfall intensity value of 200 mm/d. In addition, the simulated SR amount in the central area exhibits slight changes, while that in the surrounding areas shows substantial variations. (4) The distribution of IS and SR in the MUR of Hefei City reveals strong directional variations, which are all affected by geographical conditions. The IS coverage and SR show high positive correlation coefficients in different years. (5) The present study provides primary data for effective urban planning, water resources management and regulation, and disaster prevention and mitigation in Hefei City, as well as a scientific reference for future studies on urban IS, SR, and their quantitative relationships in other regions.

Keywords: BCI index; linear spectral mixture model; impervious surface; SCS-CN model; surface runoff; spatiotemporal evolution; the main urban region of Hefei City



Citation: Fang, G.; Li, H.; Dong, J.; Teng, H.; Pablo, R.D.A., II; Zhu, Y. Extraction and Spatiotemporal Evolution Analysis of Impervious Surface and Surface Runoff in Main Urban Region of Hefei City, China. *Sustainability* **2023**, *15*, 10537. <https://doi.org/10.3390/su151310537>

Academic Editors: Yubao Qiu, Massimo Menenti, Hongsheng Zhang, Paola De Salvo, Salvatore Gonario Pasquale Virdis, Andrea Marinoni, Dunhui Xiao and Xiyun Sun

Received: 24 May 2023

Revised: 22 June 2023

Accepted: 30 June 2023

Published: 4 July 2023



Copyright: © 2023 by the authors. Licensee MDPI, Basel, Switzerland. This article is an open access article distributed under the terms and conditions of the Creative Commons Attribution (CC BY) license (<https://creativecommons.org/licenses/by/4.0/>).

1. Introduction

Impervious surface (IS) refers to the surface covered by various building materials with extremely low water permeability of the urban underlying surface (e.g., parking lots, roads, and roofs) [1]. Compared to bare soil and vegetation surface areas, impervious surfaces are characterized by lower permeability, thereby preventing the infiltration of rainwater and, consequently, resulting in surface runoff. IS and surface runoff (SR) have been employed by several researchers worldwide to assess the quality of the urban ecological environment. Previous studies have investigated the spatiotemporal characteristics of IS and SR and their potential relationship and estimated the SR rates, promoting urban development

and planning [2]. Kauffman et al. [3] quantitatively analyzed the relationship between the base flows of 19 rivers near the University of Delaware in the United States and urban impervious surfaces, highlighting the impact of the continuous increase in urban IS on reducing the base flow of rivers. White et al. [4] investigated the effect of urbanization on changes in river runoff in coastal areas of Southern California. They indicated that increased urban impervious surfaces can lead to increased runoff during the dry season, affecting the characteristics of streams and riparian ecosystems. Verbeiren et al. [5] utilized Landsat and SPOT images to assess the impact of IS changes on rainfall runoff in the Dublin regional watershed, demonstrating the strong effect of rapid urbanization on increasing SR rates. Dams et al. [6] analyzed the spatiotemporal evolution of impervious surfaces and SR and their correlation in the Kleine Nete catchment area over the 1986–2003 period, demonstrating increases in the urban IS and SR rate by 3.8 and 9.5%, respectively. Li [7] examined the changes in the IS of the Qinhuai River Basin over the past 20 years and revealed an increase in the impervious and SR rates in the study area of about 30 and 50%, respectively. Shao and Pan [8] indicated a higher positive correlation coefficient than 0.94 between impervious and rainfall runoff rates in Xiafang Creek and Jiefang Creek in Fuzhou City. Because the IS was easily confused with the bare and sandy land, the error of extracting vegetation, soil, and IS by the linear spectral mixture model (LSMM) was relatively large. After a comparative analysis of experiments, it was confirmed that the LSMM combined with the BCI index can effectively improve the extraction accuracy of IS. Therefore, the BCI index-based LSMM is employed in this study to improve the extraction accuracy of the IS in the main urban region (MUR) of Hefei City. In addition, the Soil Conservation Service-Curve Number (SCS-CN) model is utilized in this study to simulate the SR, analyze the IS, and investigate the spatiotemporal evolution of SR to quantify the relationship between IS and SR in the study area. The simulation accuracy is evaluated using typical waterlogging points.

2. Materials and Methods

2.1. Description of the Study Area

Hefei City is located between $30^{\circ}56'$ – $32^{\circ}33'$ N and $116^{\circ}40'$ – $117^{\circ}58'$ E in the mid-latitude zone, between the central part of Anhui and the Jianghuai River (Figure 1). The study area is surrounded by mountains, lakes, rivers, and seas. Hefei City includes 4 counties (Feidong, Feixi, Changfeng, and Lujiang), 1 county-level city (Chaohu), and 4 districts (Yaohai, Luyang, Shushan, and Baohe), covering a total area of 11,445 km². Hefei City is characterized by a humid subtropical monsoon climate, with an average annual temperature, average annual precipitation, annual sunshine time, and average frost-free period of 15.7 °C, 1000 mm, 2000 h, and 228 days, respectively. Hefei City is the political, economic, cultural, transportation, financial, and commercial center of Anhui Province. In 2021, Hefei City's GDP was CNY 1141.28 billion, representing a growth of 9.2% and ranking 19th among the large and medium-sized cities in China. In this study, Hefei City was considered the study area. The main urban area includes Shushan, Luyang, Yaohai, and Baohe Districts. The slope of the study area is in a northwest–southeast direction, with an area of 1310.841 km².

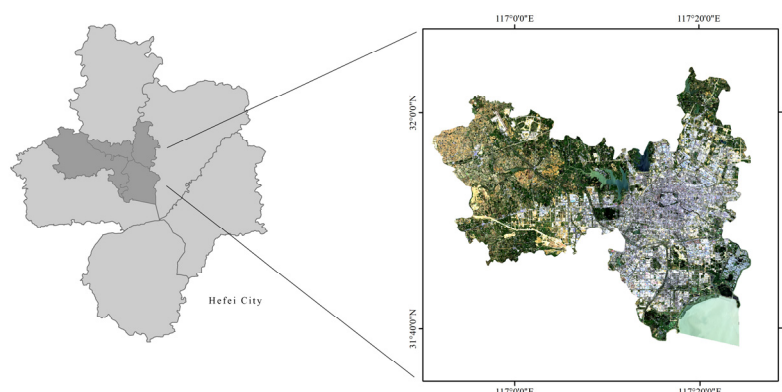


Figure 1. Geographical location of the study area.

2.2. Data Sources

2.2.1. Satellite Data

In this study, the digital elevation model data and Landsat satellite images were collected from the geospatial data cloud (<http://www.gscloud.cn>, accessed on 18 April 2022), of which the remote sensing images include 2 scenes of TM, 1 scene of ETM, and 3 scenes of OLI, with a spatial resolution of 30 m. The tracking number is 121/038, and the cloud cover of all data is below 3%. To ensure the high reliability of the experimental results, images from similar months were selected with a time interval of four years. The image attributes are listed in Table 1, while the 30 m resolution global digital elevation model data of the study area are depicted in Figure 2.

Table 1. Landsat data attributes.

Years	Image Number	Time	Cloud (%)
2001	LE71210382001141EDC00	21 May 2001	0.24
2005	LT51210382005144BJC00	24 May 2005	1.48
2009	LT51210382009123BJC00	3 May 2009	0.71
2013	LC81210382013134LGN03	14 May 2013	0.03
2017	LC81210382017113LGN00	23 April 2017	0.56
2021	LC81210382021156LGN00	5 June 2021	2.66

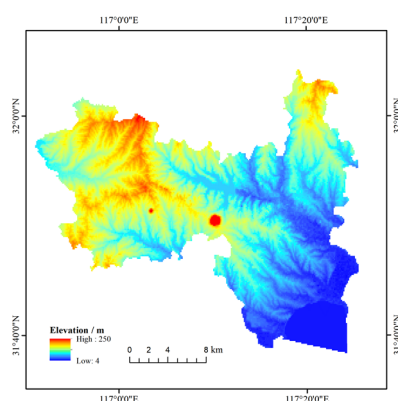


Figure 2. Elevation map of the study area.

2.2.2. Soil Data

The 1:1,000,000 soil raster data of Anhui Province were used in the present study. The soil types in the study area consist mainly of yellow–brown and paddy soils. The US Department of Agriculture Soil Conservation Service (SCS) classified soil types into four hydrologic soil groups (HSGs) (A, B, C, and D) according to their hydraulic permeability

values. The specific classification process of soil types was performed in this study based on the results by Fan et al. [9]. The classification of hydrologic soil groups in the study area is shown in Figure 3.

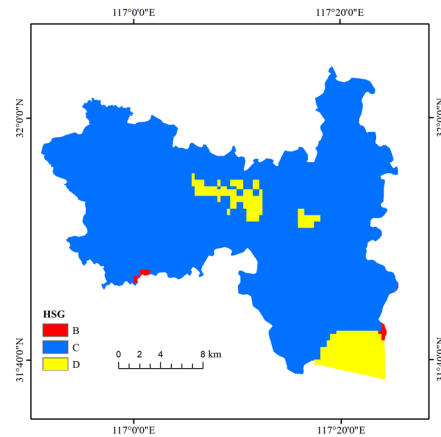


Figure 3. Hydrologic soil group in the MUR of Hefei City.

2.2.3. Precipitation Data

The maximum daily precipitation and rainfall intensity of Hefei City was 199.14 mm/d over the past 21 years. In this study, the maximum daily precipitation value of 200 mm/d was considered the unified precipitation input data for estimating the SR rates in Hefei City.

2.3. BCI Index-Based LSMM

The mathematical formula of the LSMM is Equation (1) [10,11].

$$\rho(\lambda_i) = \sum_{j=1}^n F_j \rho_j(\lambda_i) + \varepsilon(\lambda_i) \quad (1)$$

where $i = 1, 2, 3, \dots, m$ (number of bands); $j = 1, 2, 3, \dots, n$ (number of endmembers); λ_i is the wavelength of the i -th band; $\rho(\lambda_i)$ is the reflectivity of the pixel in the i -th band; F_j is the area ratio of the endmember j in the pixel; $\rho_j(\lambda_i)$ is the reflectivity of the j -endmember in the i -band; $\varepsilon(\lambda_i)$ is the residual error of the i -th band. Its constraints are Equations (2) and (3) [11].

$$\sum_{j=1}^n F_j = 1 \quad (2)$$

$$0 \leq F_j \leq 1 \quad (3)$$

Deng and Wu [12] proposed the BCI index in 2012, which consisted of three components after the tasseled cap transformation. The BCI index can be calculated using Equation (4) [12]. The principle of the BCI index is based on the fact that bright IS, dark IS, and vegetation information have high TC_1 , TC_3 , and TC_2 values, respectively [13]. Therefore, the classification of soils, vegetation, and impervious surfaces was performed in this study using the BCI index. Higher and lower BCI values than zero were classified as IS and vegetation, respectively, while BCI values close to zero were classified as soil [14].

$$BCI = \frac{\frac{TC_1 + TC_3}{2} - TC_2}{\frac{TC_1 + TC_3}{2} + TC_2} \quad (4)$$

where TC_1 , TC_2 , and TC_3 are brightness, greenness, and wetness, respectively.

Low and high albedo coverage have been commonly considered in the LSMM to obtain IS coverage. However, since the IS information is often confounded with bare soil, sandy

land, and shadow information due to the influence of human activities, the accuracy of soil, vegetation, and IS information extraction is often reduced to a certain extent. Therefore, to ensure accurate extraction information, the low albedo coverage values of the LSMM were first classified in this study into three main classes based on the BCI index, namely, low albedo IS coverage, low albedo vegetation coverage, and low albedo soil coverage, then added to the high albedo coverage, vegetation coverage, and soil coverage obtained by the LSMM. This approach can not only improve the extraction accuracy of IS information, but also decrease the impact of vegetation phenological changes on the extraction results [10].

Since the Vegetation-Impervious Surface-Soil (V-I-S) model does not consider the influence of water bodies, the modified normalized difference water index (MNDWI) [15] was first employed in this study to remove the water body information from the image data, then four endmembers were selected, as well as decomposition objects, namely, low reflectivity objects, high reflectivity objects, soil, and vegetation, to calculate the BCI index. Afterward, the IS coverage, vegetation coverage, and soil coverage were corrected. The formula of the MNDWI is Equation (5) [15].

$$MNDWI = \frac{\rho_G - \rho_{MIR}}{\rho_G + \rho_{MIR}} \quad (5)$$

where ρ_G and ρ_{MIR} are the reflectance of the green and mid-infrared bands, respectively.

2.4. Curve Number (CN) Calculation Method

2.4.1. SCS-CN Model

The SCS-CN model is a statistical empirical model developed by the US Department of SCS to estimate rainfall runoff in small watersheds. Its main objective is to determine the CN values. The total SR (Q) is calculated using Equation (6) [10].

$$Q = \begin{cases} \frac{(P - 0.2S)^2}{P + 0.8}, & P \geq 0.2S \\ 0, & P < 0.2S \end{cases} \quad (6)$$

where Q is the total runoff amount (mm); P is the total precipitation amount (mm); S is the potential water storage capacity (mm). Due to the large variation in the S values, S is calculated using Equation (7) [10].

$$S = 254 \left(\frac{100}{CN} - 1 \right) \quad (7)$$

where CN is the runoff curve parameter, ranging from 0 to 100.

2.4.2. Parameter Selection

Yao et al. [10] classified the procedure for the CN value correction proposed by Fan et al. [9] into four main steps: (1) Classifying the vegetation types based on the calculated NDVI values and assigning an initial CN value to each category regarding the TR-55 table [16]. (2) Extracting the IS, soil, and vegetation coverage using the BCI index-based LSMM. (3) Classifying the soil types into several categories and assigning an initial CN value to each category regarding the TR-55 table [16]. (4) Determining the composite CN value and simulating the SR value in the study area based on the composite CN value. To calculate the CN value of Hefei City, it was assumed that any 30×30 m area is an independent drainage area composed of IS, vegetation, and soil. The composite CN value is calculated in this study using Equation (8) [10].

$$CN = C_{ISA} \times CN_{ISA} + C_{soil} \times CN_{soil} + C_{veg} \times CN_{veg} \quad (8)$$

where CN is the composite CN value; C_{soil} , C_{veg} , and C_{ISA} are the soil, vegetation, and IS coverage, respectively, extracted by the BCI index-based LSMM; CN_{soil} , CN_{veg} , and CN_{ISA} are the initial CN value of soil, vegetation, and IS, respectively. Since the CN_{soil} values de-

pend on the soil types and soil water contents, it was assumed that all impervious surfaces, soil, and vegetation are under antecedent moisture condition (AMC) II conditions (between wet and dry soil conditions). However, under dry or wet soil conditions, adjustments to AMC I or AMC III are required. The soil classification and initial CN_{soil} values of the MUR of Hefei City are listed in Table 2.

Table 2. Soil classification and initial CN_{soil} values.

Type	Hydrological Properties	Minimum Infiltration Rate/(mm·h ⁻¹)	CN_{soil} Value
A	Thick sand, thick loess, agglomerated silt soil	7.26–11.43	77
B	Thin loess, sandy loam	3.81–7.26	86
C	Clay loam, thin sandy loam, soil with low organic matter content, soil with high clay content	1.27–3.81	91
D	Soils that swell significantly after absorbing water, plastic clays, certain saline soils	0–1.27	94

On the other hand, the classifications of IS coverage and initial CN_{ISA} in the MUR of Hefei City (Table 3) were conducted based on the results reported by Cronshey et al. [16] and Jeon et al. [17]. CN_{veg} was determined using the C_{veg} and NDVI values. The NDVI value was utilized to classify the vegetation in the study into four types, namely, grassland, farmland, trees, and others. In addition, each vegetation type was reclassified into three classes based on the C_{veg} values, namely, good, moderate, and poor, corresponding to C_{veg} values of above 0.75, between 0.5 and 0.75, and below 0.5, respectively. Vegetation classes and initial CN_{veg} values can be found in the US National Irrigation Engineering Handbook and are listed in Table 4.

Table 3. Classification of IS coverage and initial CN_{ISA} values.

IS Coverage (%)	CN_{ISA} Value			
	A	B	C	D
0–19	54	70	80	85
20–49	51	74	82	86
50–79	77	85	89	92
80–100	89	94	96	97

Note: A, B, C, and D are soil types in Table 2.

Table 4. Vegetation classification and initial CN_{veg} values.

Type	NDVI	Vegetation Coverage (C_{veg})	CN_{veg} Value			
			A	B	C	D
Others	NDVI < 0.4	—	59	74	82	86
Farmland	0.4 < NDVI < 0.57	Poor : C_{veg} < 50%	65	73	79	81
		Good : C_{veg} > 50%	61	70	77	80
Grassland	0.57 < NDVI < 0.65	Poor : C_{veg} < 50%	68	79	86	89
		Moderate : 50% < C_{veg} < 75%	49	69	79	84
Trees	NDVI > 0.65	Good : C_{veg} > 75%	39	61	74	80
		Poor : C_{veg} < 50%	48	67	77	83
		Moderate : 50% < C_{veg} < 75%	35	56	70	77
		Good : C_{veg} > 75%	30	48	65	73

Note: A, B, C, and D are soil types in Table 2.

The calibration of the SCS-CN model was conducted based on the collected rainfall and runoff data from gently sloped terrain in the United States. Therefore, the CN values

of the MUR of Hefei City were corrected in this study according to the topographic slope of 2.86% in Hefei City using Equation (9) [18]:

$$CN'' = CN \times \frac{322.79 + 15.63 \times slp}{slp + 323.52} \quad (9)$$

where CN is the CN value under AMC II conditions; CN'' is the corrected value; slp is the average slope value.

2.5. Change Analysis Method

2.5.1. Quantity Change

In this study, a quantitative analysis method was applied to investigate the change in the IS in Hefei City. The change rate (V) and change intensities (AGRs) were calculated to quantify the change in the IS in the study area using Equations (10) and (11) [10].

$$V = \frac{S_{n+i} - S_i}{n} \quad (10)$$

$$AGR = \frac{S_{n+i} - S_i}{nS_i} \times 100\% \quad (11)$$

where S_i and S_{n+i} are the area of IS in the year i and year $n + i$, respectively; n is the time interval.

2.5.2. Spatial Variation

The mean center and standard deviation ellipse (SDE) tools in ArcGIS 10.2 were employed in this study to investigate the expansion direction of the IS in the MUR of Hefei City. The calculation formulas of the mean center are Equations (12) and (13) [10].

$$\bar{X} = \frac{\sum_{i=1}^n x_i}{n} \quad (12)$$

$$\bar{Y} = \frac{\sum_{i=1}^n y_i}{n} \quad (13)$$

where x_i and y_i are the rectangular coordinates of element i ; n is the number of elements.

The SDE was proposed by Lefever [19] in 1926 to measure the distribution and direction of geographic data. This method has been widely used in ecology. The SDE mainly uses basic parameters, such as minor axis, center, and azimuth angle, to represent the spatial distribution characteristics of geographic elements [20]. The SDE ellipse center was calculated in this study using Equations (14) and (15) [10].

$$SDE_x = \sqrt{\frac{\sum_{i=1}^n (x_i - \bar{X})^2}{n}} \quad (14)$$

$$SDE_y = \sqrt{\frac{\sum_{i=1}^n (y_i - \bar{Y})^2}{n}} \quad (15)$$

where x_i and y_i are the rectangular coordinates of element i ; \bar{X} and \bar{Y} are the rectangular coordinates of the mean center; n is the number of elements.

2.6. Evaluation of Indicators

In this study, the root-mean-square error (*RMSE*), mean absolute error (*MAE*), and systematic error (*SE*) were determined to evaluate indicators. Their calculation formulas are Equations (16) through (18) [10].

$$RMSE = \sqrt{\frac{\sum_{i=1}^N (\bar{X}_i - X_i)^2}{N}} \quad (16)$$

$$SE = \frac{\sum_{i=1}^N (\bar{X}_i - X_i)^2}{N} \quad (17)$$

$$MAE = \frac{\sum_{i=1}^N |\bar{X}_i - X_i|}{N} \quad (18)$$

where \bar{X}_i is the mean proportion of IS in the sample area extracted by the BCI index-based LSMM; X_i is the proportion of IS in the sample area of the high-resolution verification image; N is the number of samples.

3. Results and Discussion

3.1. Spatiotemporal Evolution of IS

The IS, vegetation, and soil coverage in 2001, 2005, 2009, 2013, 2017, and 2021, extracted using the BCI index-based LSMM, are illustrated in Figure 4. In this study, 150 sample areas, with a size of 1×1 pixel, were first selected randomly from the MUR of Hefei City, then validated using the corresponding sample areas of the high-resolution images (2001–2009: Google Earth; 2013–2021: GaoFen-1) of the same phase in 2001–2021. The RMSE, MAE, and SE values of the LSMM and BCI index-based LSMM are listed in Table 5. The results showed lower RMSE, MAE, and SE values for the BCI index-based LSMM than those of the LSMM. In addition, the RMSE difference in 2017 was 0.16, which is better than the accuracy of results observed in 2001, 2005, 2009, 2013, and 2021.

Table 5. Accuracy comparison between LSMM and BCI index-based LSMM.

Year	RMSE		MAE		SE	
	LSMM	BCI Index-Based LSMM	LSMM	BCI Index-Based LSMM	LSMM	BCI Index-Based LSMM
2001	0.30	0.17	0.25	0.14	0.09	0.03
2005	0.27	0.15	0.22	0.12	0.07	0.02
2009	0.27	0.15	0.22	0.12	0.07	0.02
2013	0.36	0.30	0.31	0.24	0.13	0.09
2017	0.49	0.33	0.41	0.24	0.24	0.11
2021	0.29	0.26	0.24	0.19	0.08	0.06

The area, area ratio, V , and AGR of the IS in the MUR of Hefei City from 2001 to 2021 were derived and reported in Tables 6–8. The results indicated that the IS area and area ratio of the MUR of Hefei City grew from 107.555 to 387.660 km² and 8.205 to 29.573%, respectively. The V and AGR values exhibited increasing–decreasing–increasing trends. The highest V and AGR values of 24.839 km²/year and 23.094%, respectively, were observed over the 2001–2005 period. In addition, the V values over the 2001–2009 period were maintained above 6 km²/year. In contrast, substantial variations in the V and AGR values were observed between 2009 and 2021, with an overall rapid–slow expansion trend. By considering urban planning and socioeconomic factors, it was determined that Shushan and Luyang were the fastest and slowest developing districts during the period

2001–2009, with V values of 9.636 and 1.092 km²/year and AGR values of 21.264 and 22.562%, respectively. The same finding was reported between 2001 and 2009. Shushan showed V and AGR values of 9.494 km²/year and 21.264% in the 2001–2005 period and 9.636 km²/year and 11.663% in the 2005–2009 period, respectively. In contrast, Luyang showed V and AGR values of 3.464 km²/year and 22.562% during the 2001–2005 period and 1.092 km²/year and 3.739% in the 2005–2009 period, respectively. On the other hand, the fastest and slowest developing districts in the 2009–2013 period were Shushan and Baohe, with V values of 4.004 and −0.606 km²/year and AGR values of 2.067 and −0.798%, respectively. In the 2013–2017 period, the fastest and slowest developing districts were Baohe and Luyang, with V values of 3.050 and 0.053 km²/year and VGR values of 4.148 and 0.166%, respectively. In the 2017–2021 period, the fastest and slowest developing districts were Shushan and Baohe, with V values of 10.443 and −0.893 km²/year and VGR values of 7.434 and −1.042%, respectively.



Figure 4. Cont.

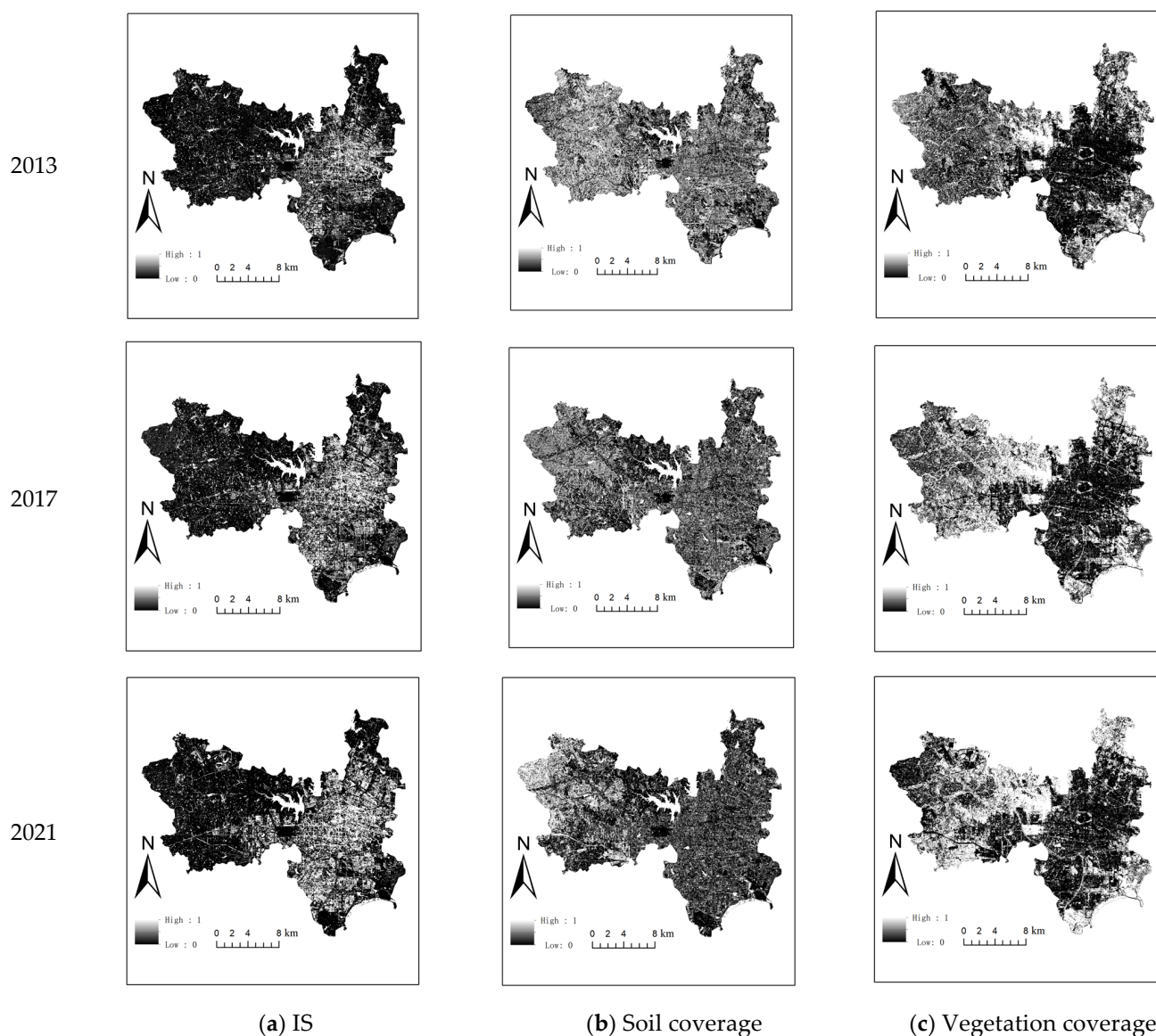


Figure 4. IS coverage, soil coverage, and vegetation coverage in the MUR of Hefei City in 2001–2021.

Table 6. Statistics of the area, area ratio, V, and AGR of IS in the study area.

Year	Area (km ²)	Area Ratio (%)	Period	V (km ² /Year)	AGR (%)
2001	107.555	8.205	2001–2005	24.839	23.094
2005	206.910	15.785	2005–2009	21.273	10.281
2009	292.001	22.276	2009–2013	6.105	2.091
2013	316.421	24.139	2013–2017	6.573	2.077
2017	342.713	26.145	2017–2021	11.237	3.279
2021	387.660	29.573	/	/	/

Table 7. V (km²/ year) and AGR (%) of IS in the study area.

	Yaohai District		Luyang District		Shushan District		Baohu District	
	V	AGR	V	AGR	V	AGR	V	AGR
2001–2005	5.3	18.346	3.464	22.562	9.494	21.264	6.586	35.239
2005–2009	2.821	5.631	1.092	3.739	9.636	11.663	7.729	17.164
2009–2013	3.169	5.163	−0.472	−1.406	4.004	2.067	−0.606	−0.798
2013–2017	2.632	3.554	0.053	0.166	0.826	0.602	3.05	4.148
2017–2021	1.418	1.676	0.285	0.892	10.443	7.434	−0.893	−1.042

Table 8. IS area (km²) and area ratio (%) of the study area.

Year	Yaohai District		Luyang District		Shushan District		Baohai District	
	Area	Area Ratio	Area	Area Ratio	Area	Area Ratio	Area	Area Ratio
2001	28.89	13.027	15.352	11.129	44.646	6.853	18.689	6.235
2005	50.091	22.586	29.207	21.173	82.62	12.682	45.032	15.024
2009	61.374	27.674	33.575	24.340	121.163	18.598	75.949	25.339
2013	74.049	33.389	31.687	22.971	137.179	21.057	73.526	24.531
2017	84.576	38.136	31.898	23.124	140.483	21.564	85.724	28.601
2021	90.247	40.693	33.036	23.949	182.255	27.976	82.151	27.409

The SDE and mean center of the IS in the study area were calculated using Equations (12) through (15) to better analyze the spatial changes in the IS in the MUR of Hefei City over the past 21 years. The results are depicted in Figure 5 and Table 9. Based on the obtained results, the SDE oblateness of the MUR of Hefei City during 2001–2021 was relatively high (over 0.380), indicating a strong directional variation in the IS of the study area. The IS is mainly distributed in Shushan District. From 2001 to 2021, the average center of the IS of the MUR of Hefei City did not change substantially and was primarily observed in Shushan District. In addition, the average center of the IS gradually moved to the southwestern part of the study area (Shushan District) from 2001. The distribution of IS was consistent with the distribution characteristics of the water system in the study area, showing a change in the expansion of IS along the flow direction of river water, demonstrating that the distribution of IS in the MUR of Hefei City was affected by reported hydrological conditions. In 2005, 2009, and 2013, the short radius of the SDE was higher than 6.126 km, indicating that the distribution of impervious surfaces in the study area in these years was relatively scattered. The short radius in 2021 was 5.810 km, indicating a more concentrated IS distribution than in other years.

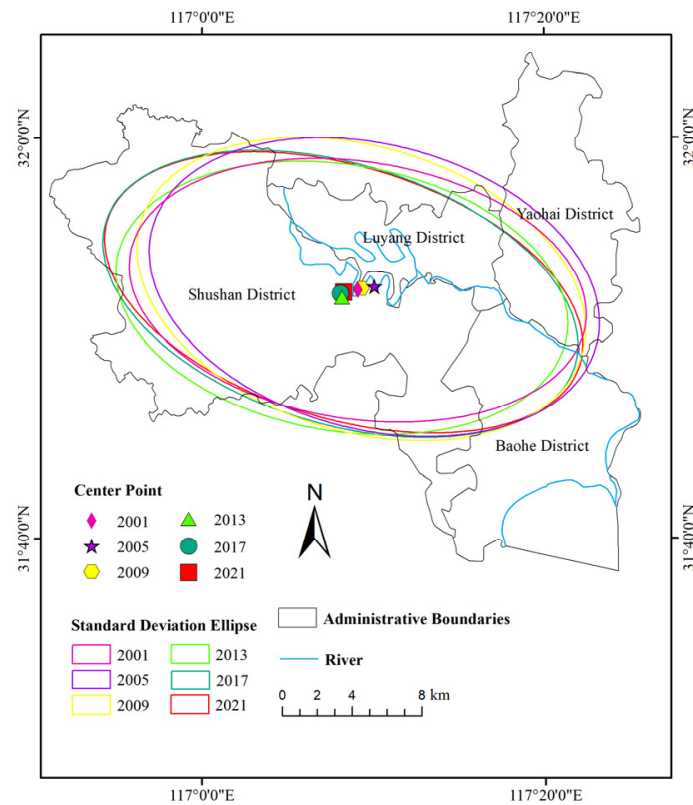


Figure 5. SDE and center point of IS in the study area in 2001–2021.

Table 9. SDE parameters of IS in the study area.

Year	Deflection Angle (°)	Long Radius (km)	Short Radius (km)	Oblateness ((Long Radius-Short Radius)/Long Radius)	Mean Center Coordinates
2001	98.696	10.614	5.922	0.442	117°9.10' E, 31°52.39' N
2005	104.645	10.584	6.560	0.380	117°10.06' E, 31°52.55' N
2009	106.807	10.616	6.563	0.382	117°9.30' E, 31°52.46' N
2013	99.782	10.512	6.126	0.417	117°8.17' E, 31°52.01' N
2017	107.066	11.302	5.986	0.470	117°8.08' E, 31°52.21' N
2021	106.951	11.386	5.810	0.490	117°8.27' E, 31°52.29' N

3.2. Spatiotemporal Evolution Analysis of SR

The BCI index-based LSMM was utilized in this study to extract the IS, soil, and vegetation coverage of the MUR of Hefei City. The extracted results were used as inputs to determine the CN value of the MUR of Hefei City using Equation (9). Since water bodies were neglected in the CN calculation, the CN value of the water body was set to 98, according to Fan et al. [7]. As illustrated in Figure 6, areas with CN values higher than 90 are mainly distributed in the Baohe and Yaohai districts, where the IS coverage and density are relatively high and soil/vegetation coverage is relatively low. On the other hand, the areas with CN values below 90 are mainly distributed in the Shushan and Luyang districts, where the IS and soil/vegetation coverage are relatively low and high, respectively.

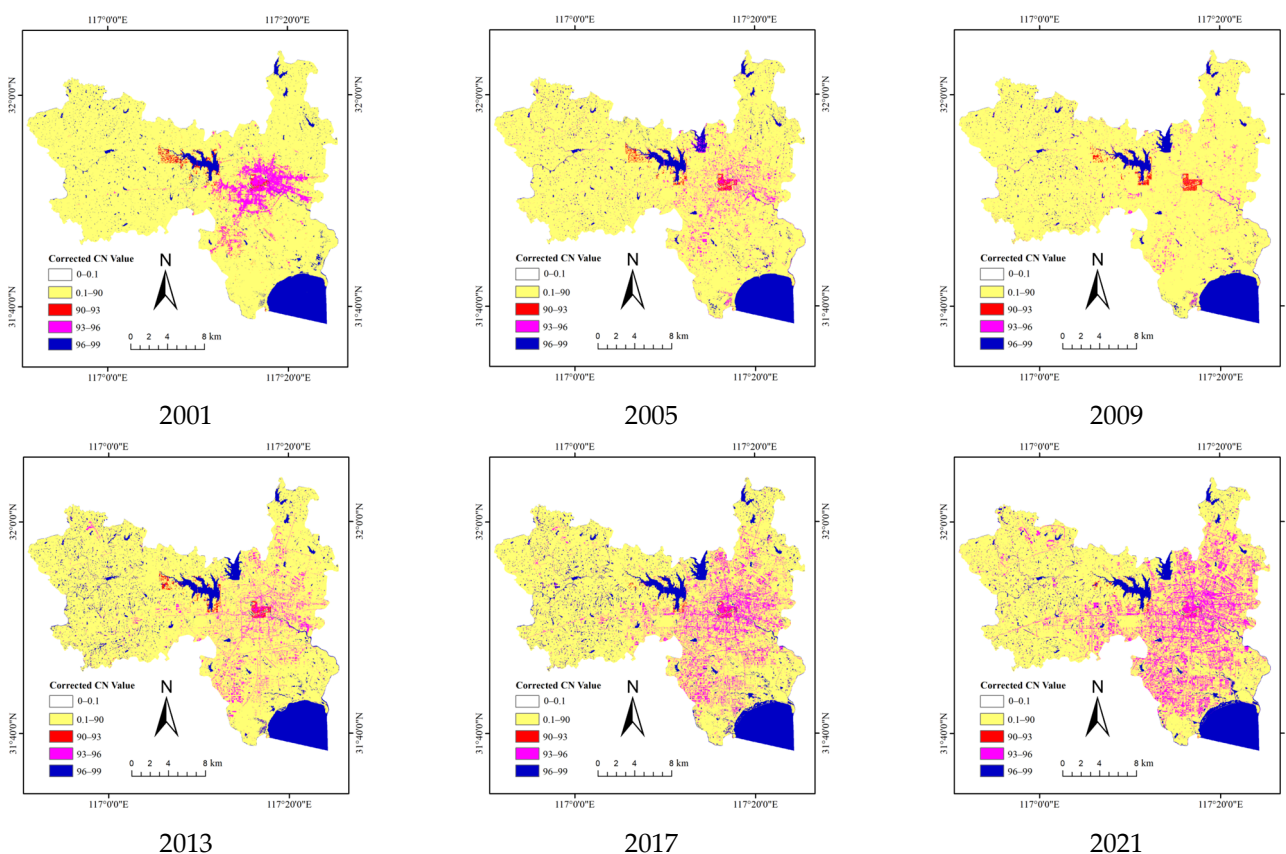


Figure 6. Synthetic CN values of the study area in 2001–2021.

The precipitation intensity of 200 mm/d was employed as the input data to estimate SR in the MUR of Hefei City between 2001 and 2021 using Equations (6) and (7) to better understand the distribution of SR in the MUR of Hefei City. Figure 7 shows that the SR in the MUR of Hefei City during the 2001–2021 period at the rainfall intensity value of 200 mm/d ranged from 165 to 195 mm, showing a continuous increase from the city center to the surrounding areas. The magenta areas became increasingly larger, indicating a continuous increase in the simulated SR in the main urban area of Hefei City. In addition, the simulated SR in the central and surrounding areas of Hefei City exhibited slight and substantial changes, respectively. Sixteen typical waterlogging points were selected from the MUR of Hefei City in June 2021 from media, periodicals, newspapers, and other materials (Figure 7) to evaluate the accuracy of the simulated SR. Based on the obtained results, the typical waterlogging points were located in areas with high simulated SR values (above 165 mm), exhibiting a high correlation between the waterlogging points and high-value areas in the extracted SR distribution map, thereby indicating a good simulation accuracy of the SR values.

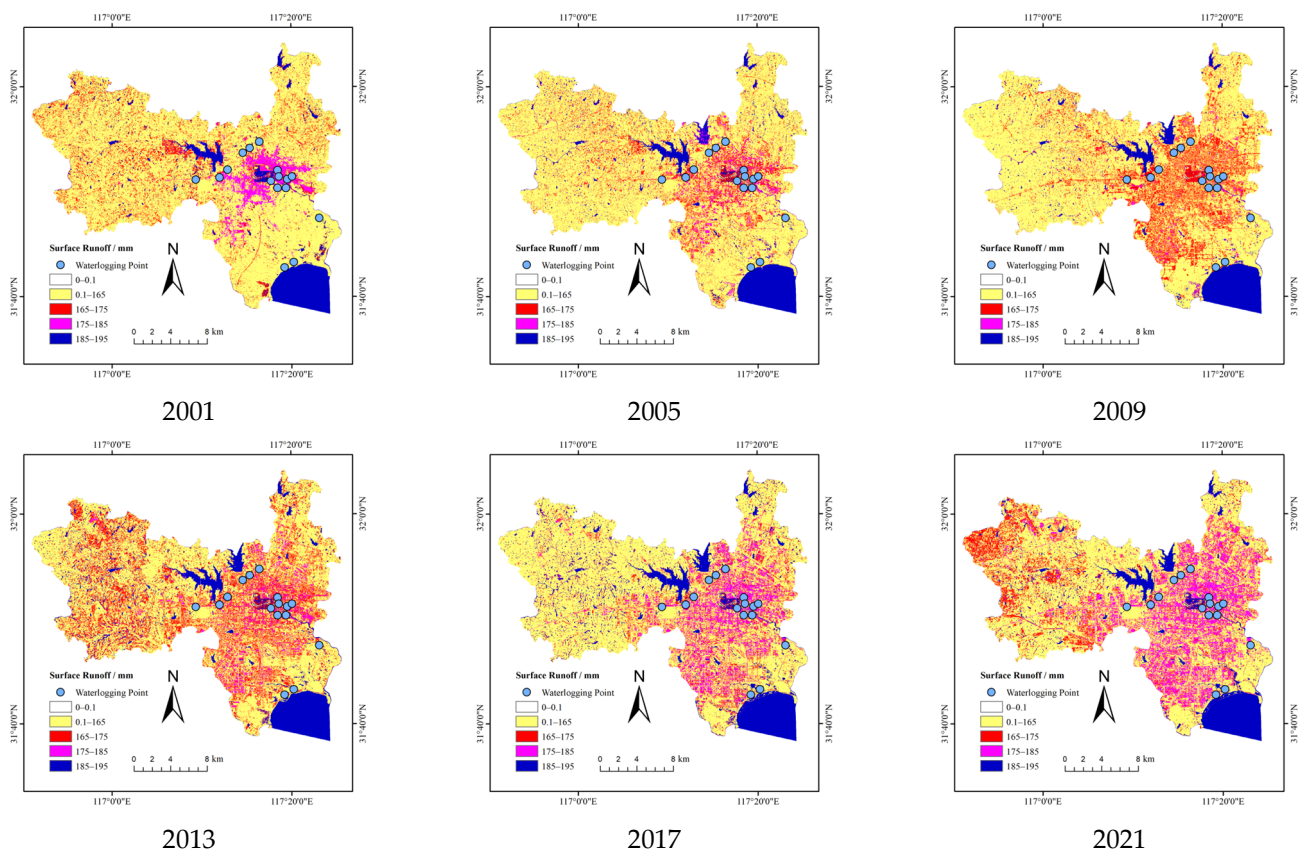


Figure 7. Typical waterlogging points and SR values in the study area in 2001–2021.

The SDE and mean center were calculated for the SR range of 165–195 mm using Equations (12) through (15) to better analyze the spatial variation of SR in the MUR of Hefei City over the past 21 years. The obtained results are shown in Figure 8 and Table 10. The SDE oblateness in the study area in 2009 was 0.379, while that in the remaining years was relatively high (above 0.384), indicating a strong directional variation in the 165–195 mm SR area, which was roughly distributed in the northeast–northwest direction, including most of the water systems. This finding indicated that the distribution of the 165–195 mm SR was affected by the geographical conditions of Hefei City. In addition, the average center of SR of the 165–195 mm SR in the MUR of Hefei City did not vary substantially between 2001 and 2021. The average center was mainly located in the Shushan District, indicating that Shushan District had a large SR and was susceptible to flooding during heavy rainfall

events. Due to the high slope degrees in the Shushan, Luyang, and Baohe districts, these districts were also be prone to flooding. Since 2001, the average center of the 165–195 mm SR has gradually moved to the northeastern and northwestern parts of the study area.

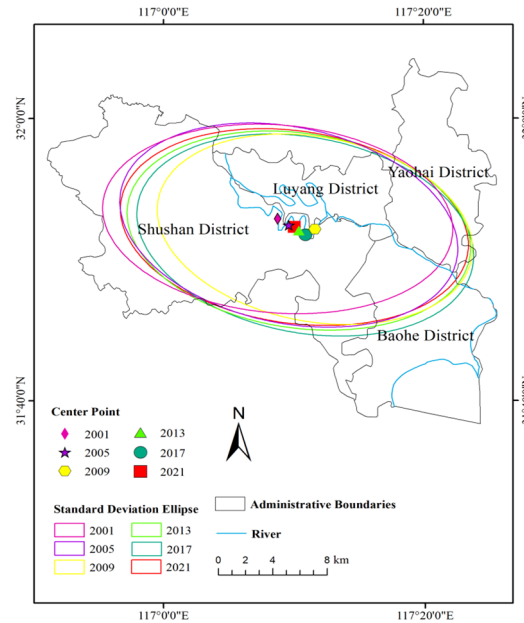


Figure 8. SDE and mean center of 165–195 mm SR in the MUR of Hefei City in 2001–2021.

Table 10. SDE parameters of 165–195 mm SR area.

Year	Deflection Angle (°)	Long Radius (km)	Short Radius (km)	Oblateness ((Long Radius-Short Radius)/Long Radius)	Mean Center Coordinates
2001	95.719	10.633	6.142	0.422	117°8.77' E, 31°52.89' N
2005	103.878	10.417	6.383	0.387	117°9.63' E, 31°52.45' N
2009	102.537	9.683	6.013	0.379	117°11.63' E, 31°52.15' N
2013	99.973	10.494	6.355	0.394	117°10.40' E, 31°52.06' N
2017	102.509	10.345	6.374	0.384	117°10.89' E, 31°51.75' N
2021	99.837	10.634	6.271	0.410	117°10.06' E, 31°52.31' N

3.3. Correlation and Regression Analysis of Impervious Coverage and SR

3.3.1. Correlation Analysis

The obtained results indicated a close relationship between the SR and IS in the MUR of Hefei City. The correlation analysis of the IS and SR in the study area was conducted to further quantify the relationship between SR and IS. To ensure the reliability and accuracy of data analysis, the study area was first divided into 4 regions, including Yaohai District, Luyang District, Shushan District, and Baohe District, based on the local administrative divisions, and then 200 sample points (1 × 1 pixel) were randomly selected for correlation analysis. The obtained results showed that the correlation coefficients (Rs) between SR and IS in the MUR of Hefei City in 2001, 2005, 2009, 2013, 2017, and 2021 were 0.890, 0.676, 0.753, 0.657, 0.773, and 0.818, respectively.

3.3.2. Regression Analysis

In this study, a regression analysis was performed to quantify the relationship between IS and SR in the MUR of Hefei City. Figure 9 exhibits significant correlations between the IS and SR in the MUR of Hefei City from 2001 to 2021. The correlation coefficients between the IS and SR are 0.946, 0.886, 0.902, 0.871, 0.912, and 0.910 in 2001, 2005, 2009, 2013, 2017, and 2021 respectively. In addition, the results revealed decreasing and increasing trends in SR at IS between 0% and 30% and over 30%, respectively. Therefore, it is crucial to maintain an IS below 30% to reduce SR and ensure effective control of urban flooding.

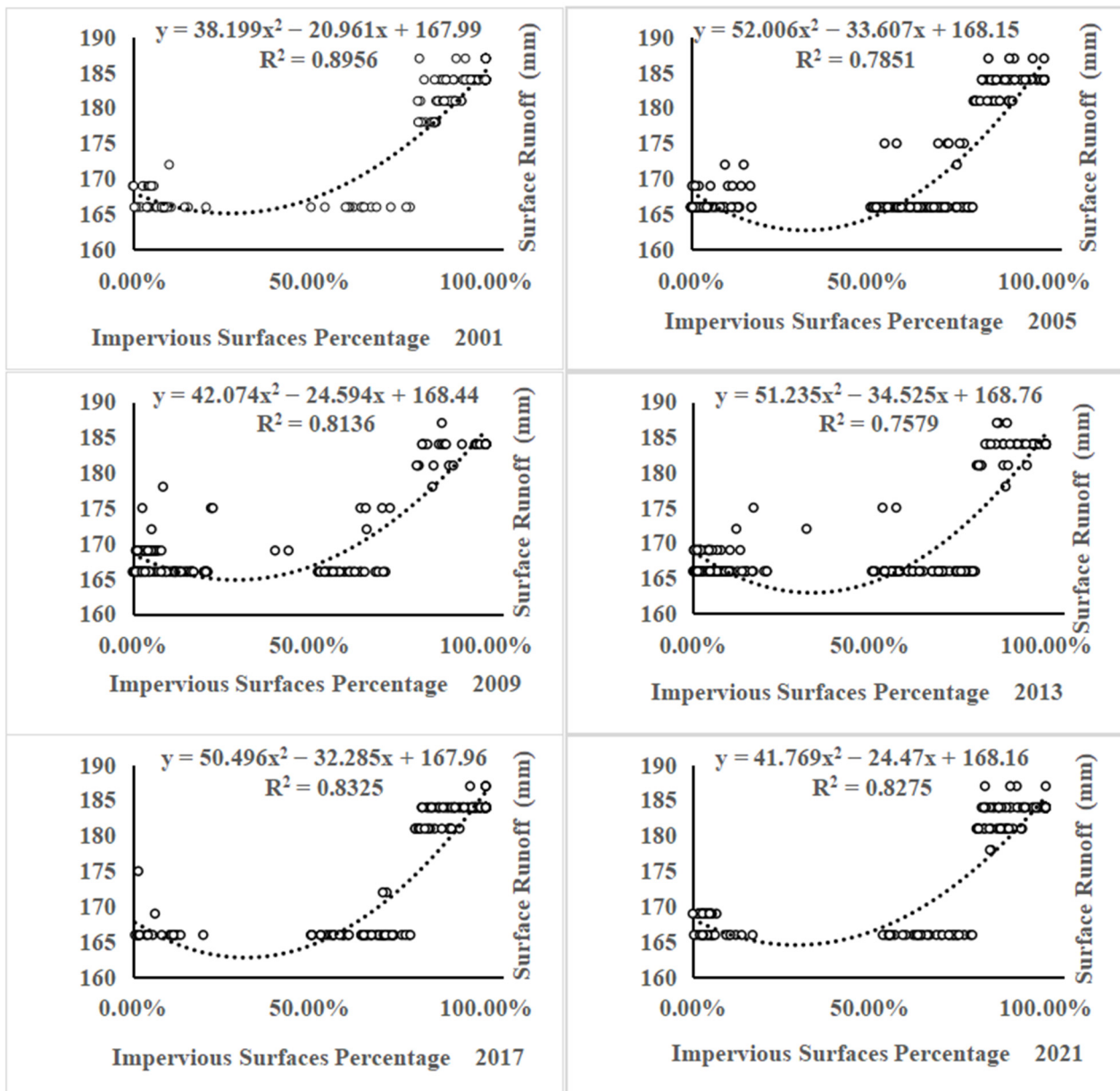


Figure 9. Regression analysis of impervious coverage and SR.

4. Conclusions

- (1) The study's results demonstrated the effectiveness of the BCI index-based LSMM in extracting the IS, vegetation, and soil coverage of the MUR of Hefei City. The SCS-CN model was utilized to simulate the SR in the MUR of Hefei City. The simulation accuracy was evaluated using typical waterlogging points and proved good.

- (2) The IS area in the MUR of Hefei City showed an upward trend from 2001 to 2021. The V and the AGR values exhibited increasing–decreasing–increasing trends. The highest V and AGR values were observed between 2001 and 2005. The distribution of impervious surfaces displayed strong directional variation and was relatively concentrated in Shushan District. The average center of the IS did not vary significantly from 2001 to 2021, showing a gradual movement towards the southwestern part of the study area (Shushan District).
- (3) At a rainfall intensity value of 200 mm/d, the SR (165–195 mm) in the MUR of Hefei City revealed a continuous expansion from the city center to the surrounding areas of the study area between 2001 and 2021. In addition, the typical waterlogging points were located in areas with high simulated SR values (above 165 mm). The average center of SR for 2001–2021 did not reveal considerable changes, showing a gradual movement towards the northeastern and northwestern parts of the study area and being primarily distributed in the Shushan District.
- (4) There were positive correlations between the impervious coverage and SR in the MUR of Hefei City over the studied period. Based on the study's results, it is crucial to maintain an IS below 30% in Hefei City to reduce SR amounts and ensure effective control of urban flooding.
- (5) The findings can provide a reference for optimizing the spatial pattern of urban impervious surfaces and controlling SR.
- (6) Due to a lack of measured SR data in the MUR of Hefei City, field verification is insufficient. In future research, the authors will fully consider the measured SR data and urban drainage network data to make the research results and methods more practical and scientific.

Author Contributions: Conceptualization, G.F., H.L. and R.D.A.P.II; methodology, G.F., H.L. and H.T.; software, H.L. and H.T.; validation, G.F., H.L. and H.T.; formal analysis, G.F.; resources, H.L. and J.D.; data curation, J.D.; writing—original draft preparation, G.F., J.D. and Y.Z.; writing—review and editing, G.F., H.L., J.D. and R.D.A.P.II; visualization, Y.Z. and J.D.; supervision, G.F. and H.L.; project administration, H.L.; funding acquisition, G.F. All authors have read and agreed to the published version of the manuscript.

Funding: This research was funded by the Scientific Research Development Fund of Suzhou University (2021fzjj23), 3S Technology Application Research Center in Northern Anhui (2021XJPT12), Teaching Team of Surveying and Mapping Engineering in Anhui Province (2020jxt285), Professional Leader Fund of Suzhou University (2019XJZY06), and School-enterprise Cooperation Practice Education Base of Suzhou University (szxy2022xqhz01).

Institutional Review Board Statement: Not applicable.

Informed Consent Statement: Not applicable.

Data Availability Statement: The authors confirm that all the data are available in the article.

Conflicts of Interest: The authors declare no conflict of interest.

References

1. Xu, H.Q. A new remote sensing index for fastly extracting impervious surface information. *Geomat. Inf. Sci. Wuhan Univ.* **2008**, *11*, 1150–1153.
2. Liu, R.Y. Remote Sensing Estimation and Spatiotemporal Evolution Analysis of Urban Surface Runoff in Xuzhou Based on Impervious Surface. Master's Thesis, China University of Mining and Technology, Xuzhou, China, 2022.
3. Kauffman, G.J.; Belden, A.C.; Vonck, K.J.; Homsey, A.R. Link between impervious cover and base flow in the White Clay Creek Wild and Scenic Watershed in Delaware. *J. Hydrol. Eng.* **2009**, *4*, 324–335.
4. White, M.D.; Greer, K.A. The effects of watershed urbanization on the stream hydrology and riparian vegetation of Los Peñasquitos Creek, California. *Landscape Urban Plan.* **2006**, *2*, 125–138.
5. Verbeiren, B.; Van De Voorde, T.; Canters, F.; Binard, M.; Cornet, Y.; Batelaan, O. Assessing urbanisation effects on rainfall-runoff using a remote sensing supported modelling strategy. *Int. J. Appl. Earth Obs. Geoinf.* **2013**, *21*, 92–102.
6. Dams, J.; Dujardin, J.; Reggers, R.; Bashir, I.; Canters, F.; Batelaan, O. Mapping impervious surface change from remote sensing for hydrological modeling. *J. Hydrol.* **2013**, *485*, 84–95.

7. Li, C.L. The Extract Impervious Surface and Its Effect on Hydrological on the Qinhuai River Basin. Master's Thesis, Nanjing University, Nanjing, China, 2011.
8. Shao, W.; Pan, W.B. On the relationship between urban impervious surface and rainfall-runoff. *J. Subtrop. Resour. Environ.* **2012**, *4*, 20–27.
9. Fan, F.L.; Deng, Y.B.; Hu, X.F.; Weng, Q.H. Estimating composite curve number using an improved SCS-CN method with remotely sensed variables in Guangzhou, China. *Remote Sens.* **2013**, *3*, 1425–1438.
10. Yao, Z.X.; Meng, Q.Y.; Sun, Z.H.; Liu, S.F.; Zhang, L.L. Temporal and spatial correlation between impervious surface and surface runoff: A case study of the main urban area of Hangzhou city. *J. Remote Sens. Chin.* **2020**, *2*, 182–198.
11. Yue, W.Z.; Wu, C.F. Urban impervious surface distribution estimation by spectral mixture analysis. *J. Remote Sens.* **2007**, *6*, 914–922.
12. Deng, C.B.; Wu, C.S. BCI: A biophysical composition index for remote sensing of urban environments. *Remote Sens. Environ.* **2012**, *127*, 247–259.
13. Xu, H.Q.; Wang, M.Y. Remote sensing-based retrieval of ground impervious surfaces. *J. Remote Sens.* **2016**, *5*, 1270–1289.
14. Li, P.; Wang, Y.J.; Xing, W.J.; Chen, Y.H. Application of urban impervious surface extraction based on TM image—Taking Guangzhou City as an example. *J. Heilongjiang Inst. Technol.* **2016**, *1*, 19–23.
15. Xu, H.Q. A study on information extraction of water body with the modified normalized difference water index (MNDWI). *J. Remote Sens.* **2005**, *5*, 589–595.
16. Cronshey, R.G.; Roberts, R.T.; Miller, N. *Urban Hydrology for Small Watersheds (TR-55 REV.)*; American Society of Civil Engineers: Reston, VA, USA, 1985; pp. 1268–1273.
17. Jeon, J.H.; Lim, K.; Engel, B. Regional calibration of SCS-CN L-THIA model: Application for ungauged basins. *Water* **2014**, *5*, 1339–1359.
18. Huang, M.B.; Gallichand, J.; Wang, Z.L.; Goulet, M. A modification to the soil conservation service curve number method for steep slopes in the Loess Plateau of China. *Hydrol. Process* **2006**, *3*, 579–589.
19. Lefever, D.W. Measuring geographic concentration by means of the standard deviational ellipse. *Am. J. Sociol.* **1926**, *1*, 88–94.
20. Zhao, L.; Zhao, Z.Q. Projecting the spatial variation of economic based on the specific ellipses in China. *Sci. Geogr. Sin.* **2014**, *8*, 979–986.

Disclaimer/Publisher's Note: The statements, opinions and data contained in all publications are solely those of the individual author(s) and contributor(s) and not of MDPI and/or the editor(s). MDPI and/or the editor(s) disclaim responsibility for any injury to people or property resulting from any ideas, methods, instructions or products referred to in the content.